Jerzy FIOŁKA

Silesian University of Technology
ORCID: 0000-0003-0551-6746

doi:10.15199/48.2022.06.08

Application of the discrete linear chirp transform (DLCT) to estimate the parameters of multicomponent LFM signals

Abstract. *This paper is focused on method to estimate the parameters of multicomponent linear frequency modulation (LFM) signals. These non-stationary signals, which are often referred to as "chirp", are encountered in many fields such as communication, vibration analysis, radar systems. The presented method, which is based on the discrete linear chirp transform (DLCT), permits the chirp parameters to be precisely estimated. Its high performance, which was proven by the simulation results, coupled with its simplicity, makes this method useful for many applications.*

Streszczenie. *W artykule przedstawiono metodę estymacji parametrów wieloskładnikowych sygnałów z liniową modulacją częstotliwości. Z tego typu sygnałami mamy do czynienia w takich dziedzinach jak telekomunikacja, analiza drgań, systemy radarowe. Przedstawiona metoda, bazująca na DLCT (ang. Discrete linear chirp transform), pozwala na oszacowanie parametrów wspomnianych sygnałów. Jej wysoka skuteczność, potwierdzona wynikami symulacji, w połączeniu z prostotą, czyni metodę użyteczną w wielu zastosowaniach. (**Zastosowanie transformacji DLCT do estymacji wartości parametrów wieloskładnikowych sygnałów LFM**).*

Keywords: non-stationary signal analysis, signal processing, time-frequency analysis.
Słowa kluczowe: analiza sygnałów niestacjonarnych, przetwarzanie sygnałów, analiza czasowo-częstotliwościowa.

Introduction

Chirp-type signals are common in many areas such as physics, seismic exploration, communication, radar-based object detection systems etc. Many phenomena can be explained by analysing the chirp parameters. For example, in synthetic aperture radar (SAR) imaging, the chirp rate in the radar return signal provides information about a moving target. The traditional Fourier transform is not suitable for processing those types of signals, and therefore various methods have been proposed.

Estimating the chirp parameters has been of interest for quite some time. Many of the methods that have proposed in the literature are based on the maximum likelihood principle. These estimators give the optimal solution but are difficult to implement because it requires the computationally expensive numerical optimisation of nonlinear cost functions, which have many local extrema. Moreover, a necessary condition for using this approach is a high signal-to-noise ratio of the analysed signals [1]. For these reasons, many suboptimal solutions have been proposed, e.g. [2, 3].

An alternative approach for analysing the LFM signals originated with the development of time-frequency distributions (TFD). The commonly known Wigner distribution (WD) represents a linear chirp in an ideal way, i.e., as a straight line on the time-frequency (T-F) plane. Thus, by studying the plane, we are able to easily determine the chirp parameters. However, for multicomponent signals, their bilinear structure produces undesirable oscillatory interferences that are known as cross-terms, which is a fundamental limitation to the applicability of the quadratic time-frequency methods. Because cross-terms render the TFD difficult to interpret (especially when there are numerous components), many alternative distributions have been proposed in the literature [4, 5]. Some of the best-known are the Choi-Williams (CW), pseudo-Wigner-Ville (PWV), Born-Jordan (BJ) and reduced interference (RI) distribution. However, it is worth noting that a consequence of suppressing cross-terms is that many useful properties of the distribution are lost (e.g., frequency-support conservation, unitarity). Thus, there is a trade-off between the readability of the T-F representation and the number of desirable properties. Moreover, the efficiency of a particular distribution depends on the nature of the analysed waveforms. Another disadvantage of these methods is also their high computational complexity.

In contrast to the bilinear TFDs, which provide information about the energy distribution on the T-F plane, linear time-frequency representations decompose a signal to its elementary components (the atoms). Among the possible representations, the short-time Fourier transform (STFT) is the one that is best known. The advantage of this approach is undoubtedly its linearity and easiness of implementation. However, it also suffers from a trade-off between the time and frequency resolution, which disturbs the readability of the time-frequency representation, and therefore also reduces the accuracy of reading the chirp parameters.

Recently, adaptive methods for processing multicomponent, non-stationary signals have become of great interest. The basic idea of these approaches is to use a signal-dependent basis to decompose the original signal into a series of oscillatory components (modes). The empirical mode decomposition (EMD), which was proposed by Huang et al., is a well-known example of this approach [6]. EMD is able to decompose a multicomponent signal into a set of complete orthogonal intrinsic mode functions (IMFs) using basis functions that are derived from the signal itself. After the signal has decomposed, the further signal processing operations can be performed separately on each component. This enables the Hilbert transform to be used to determine the instantaneous frequency and amplitude in order to characterise the analysed signal. Some important limitations that should be kept in mind are that EMD suffers from mode mixing, the unclear physical meaning of individual IMFs, a sensitivity to noise and a lack of a mathematical theory [6, 7].

The estimation problem discussed here was also addressed in [8, 9] Using the fractional Fourier transform (FrFT), it is possible to rotate the signal in the T-F plane [10]. By setting the fractional order α of FrFT to the value that corresponds to the spare representation of the analysed signal, the chirp rate can easily be obtained using the connection between the chirp rate and α. Although it has been introduced in many papers as a tool for processing chirp signals in applications such as radar and sonar, automotive, bioacoustics etc., the ability of the FrFT to deal with real-world signals is limited [11, 12, 13].

Moreover, this approach becomes inefficient when more than one chirp is being considered [14].

This paper also focuses on the problem of estimating the parameters of multicomponent linear chirp signals. The presented approach is based on the discrete linear chirp transform (DLCT). The DLCT, which was introduced in [14] in the context of data compression, can represent any signal in terms of linear chirps. Using this tool, it is possible to transform a non-sparse signal in the T-F plane into a sparse signal in the time or frequency domain. Then, by finding the peaks in the three-dimensional plot of the magnitude of the DLCT, the parameters of the chirp or combination of chirps can be determined using this transform. To confirm the usefulness of the DLCT for solving the estimation problem, numerical simulations with both synthetic and real signals were conducted.

Signal model

A multicomponent signal can be modelled as the sum of the monocomponent signals

$$s(t)=\sum_{k=1}^{K} s_k(t) \tag{1}$$

where K is the number of the signal components.

Let $z_k(t)$ denote the analytic associate of the signal's k-th component

$$z_k(t)=s_k(t)+jH\left[s_k(t)\right]=a_k(t)e^{j\varphi_k(t)} \tag{2}$$

where H is the Hilbert transform and the $a_k(t)$ is the instantaneous amplitude (IA).
The instantaneous frequency (IF) of each component is defined by the derivative of the phase of $z_k(t)$

$$f_k(t)=\frac{1}{2\pi}\frac{d\varphi_k(t)}{dt} \tag{3}$$

For a linear chirp, the phase changes as

$$\varphi(t)=2\pi(\chi t^2+\gamma t) \tag{4}$$

where χ, γ are respectively, the chirp rate and the initial frequency of a continuous chirp. Thus, using (3) the IF is given by

$$f(t)=2\chi t+\gamma \tag{5}$$

The discrete linear chirp transform

The DLCT, which was proposed in [14], can represent any signal in terms of linear chirps. This representation, which generalises the discrete Fourier transform (DFT), can be used to determine the parameters of a chirp (or a combination of chirps) [11].

A building block of the DLCT is a discrete-time linear chirp with finite support, $0\le n\le N$-1,

$$\phi_{\beta,k}(n)=\exp\left(j\frac{2\pi}{N}(\beta n^2+kn)\right) \tag{6}$$

where β is the chirp rate and k is the initial frequency [14].
Let us now assume that β has a finite support, $-\Lambda\le\beta\le\Lambda$. According to [14]

$$\int_{-\Lambda}^{+\Lambda}\sum_{n=0}^{N-1}\phi_{\beta,k}(n)\phi^*_{\beta,m}(n)d\beta=\int_{-\Lambda}^{+\Lambda}N\delta(k-m)d\beta= \tag{7}$$
$$=2\Lambda N\delta(k-m)$$

we can construct an orthonormal basis $\{\phi_{\beta,k}(n)\}$ with respect to k in the support of β and n. Thus, the linear chirp representation of the signal $x(n)$, $0\le n\le N$-1, can be written as

$$x(n)=\int_{-\Lambda}^{+\Lambda}\sum_{k=0}^{N-1}\frac{X(k,\beta)}{N}\exp\left(j\frac{2\pi}{N}((\beta n+k)n)\right)d\beta \tag{8}$$

Using the orthogonality of the basis, the expansion coefficients in (8) can be computed as [14]

$$X(k,\beta)=\sum_{n=0}^{N-1}x(n)\exp\left(-j\frac{2\pi}{N}(\beta n^2+kn)\right) \tag{9}$$

To obtain a discrete representation, the β must be discretised [11]. This can be done by defining parameter

$$C=\frac{2\Lambda}{L} \tag{10}$$

which leads to the following approximation

$$\beta\approx lC \tag{11}$$

with integer-valued l

$$-\frac{L}{2}\le l\le\frac{L}{2}-1 \tag{12}$$

The integer value of L can be arbitrary (increasing L increases the chirp rate detection resolution).
Finally, the discrete linear chirp transform can be written as [11,14]

$$X(k,l)=\sum_{n=0}^{N-1}x(n)\exp\left(-j\frac{2\pi}{N}(lCn^2+kn)\right) \tag{13}$$

whereas the inverse DLCT can be written as

$$x(n)=\sum_{l=-L/2}^{L/2-1}\sum_{k=0}^{N-1}\frac{X(k,l)}{LN}\exp\left(j\frac{2\pi}{N}(lCn^2+kn)\right) \tag{14}$$

where

$$0\le n,k\le N-1$$
$$-\frac{L}{2}\le l\le\frac{L}{2}-1 \tag{15}$$

Efficient implementation of the DLCT using FFT

One of the advantages of the DLCT is that it can be effectively implemented using the fast Fourier transform (FFT) algorithm. The equation (13) can be written in terms of the DFT notation as [11,14]

(16)

$$X(k,l)=\sum_{n=0}^{N-1}\underbrace{\left[x(n)e^{-j2\pi lCn^2/N}\right]}_{h(n,l)}e^{-j2\pi kn/N}$$

Thus, for each fixed l_0, $X(k,l_0)$ is the DFT of $h(n,l_0)$. The above reasoning can also be applied to an inverse DLCT

(17)

$$x(n)=\frac{1}{L}\sum_{l=-L/2}^{L/2-1}\underbrace{\left[\sum_{k=0}^{N-1}\frac{X(k,l)}{N}e^{j2\pi kn/N}\right]}_{g(n,l)}e^{j2\pi lCn^2/N}$$

recognising the application of an inverse DFT to the expansion coefficients, where $g(n,l)$ is computed for each l_0 that satisfies $-L/2 \le l_0 \le L/2-1$.

Sampling of the linear chirp signal

To establish the connection between the parameters of a discrete and continuous chirp, let's consider a uniform sampling $t=nT_s$ with a sampling period $T_s=1/f_s$ and f_s is the sampling frequency. For a continuous chirp of the form

(18) $$x(t)=e^{j2\pi(\chi t^2+\gamma t)}$$

the discretisation leads to

(19)

$$x(nT_s)=\exp\left(j2\pi(\chi n^2T_s^2+\gamma nT_s)\right)=$$
$$=\exp\left(j\frac{2\pi}{N}(\chi T_s^2Nn^2+\gamma T_sNn)\right)$$

Comparing (19) with (6) yields the sought relationships between the parameters of the continuous and discrete chirps

(20) $$\chi T_s^2N=\beta$$

and

(21) $$\gamma T_sN=k$$

Simulation results

To illustrate how the method works, computer experiments were conducted out on a synthetic and a real-world signal (an in-cylinder pressure waveform that had been recorded for abnormal combustion in a spark-ignition engine).

Experiment 1: To evaluate the performance of the DLCT in estimating the chirp parameters, we ran a simulation for a multicomponent, complex signal

(22)

$$x(t)=e^{j2\pi(\chi_1t^2+\gamma_1t)}+e^{j2\pi(\chi_2t^2+\gamma_2t)}+e^{j2\pi(\chi_3t^2+\gamma_3t)}$$

with the following parameters values: χ_1=5000 Hz/s, γ_1=1 kHz; χ_2=-5000 Hz/s, γ_2=2 kHz; χ_3=2500 Hz/s, γ_3=4 kHz. The signal was sampled at f_s=10 kHz and the length was N= 1000. Figure 1 shows the three-dimensional plot of the $|DLCT|^2$. At the locations (χ_1, γ_1)=(5000 Hz/s, 1 kHz), (χ_2, γ_2)=(-5000 Hz/s, 2 kHz), (χ_3, γ_3)=(2500 Hz/s, 4 kHz) there are clearly visible peaks that correspond to the three chirps. One can see that obtained results are identical to the expected values.

Experiment 2: Knocking combustion in spark-ignition (SI) engines is an unwanted form of combustion. It reduces engine durability, power density, fuel consumption as well as emission performance [15]. Several methods can be used to detect this phenomenon [16]. One of them is based on the direct measurement and analysis of the in-cylinder pressure [17, 18, 19].

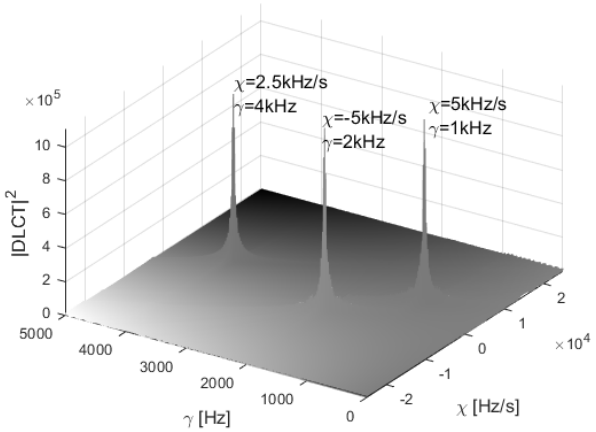

Fig.1. Three-dimensional plot of the $|DLCT|^2$ for the synthetic signal

During knocking, high-frequency pressure fluctuations whose instantaneous frequency and amplitude decrease over time is observed. In the knock window (crank angle range starting from near the top dead centre and ending about 70° after the top dead centre), the pressure waveform can be viewed as a multicomponent, linear (or near-linear) frequency modulation signal, which is embedded in the background noise. Since the pressure signal exhibits time-varying spectra, the natural choice is to use the time-frequency plane to study it. As an example, Figure 2 shows the Choi-Williams distribution of a pressure signal for a knocking cycle. As can be seen, during knocking, four resonance frequencies, which were located in the range of 6 kHz - 20 kHz, were observed.

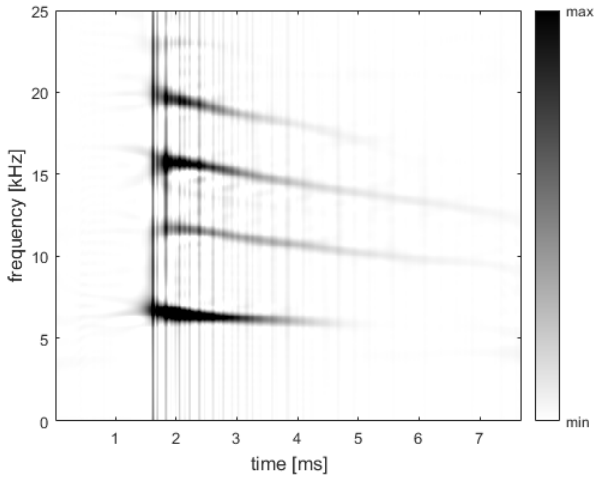

Fig.2. The Choi-Williams distribution of a cylinder pressure trace for a knocking combustion cycle

The above pressure signal was used to illustrate how the DLCT works with real-world data. On the DLCT plot, which is presented in Figure 3, four peaks that correspond to resonance frequencies shown in Figure 2 can be identified. To increase the readability of the representation, the obtained values of the $|DLCT|^2$ were thresholded (values lower than $0.1\cdot|\text{DLCT}|^2_{\text{max}}$ were set to zero). The

parameters of the chirps that were determined using the DLCT were

- (χ_1,γ_1)=(-84771 Hz/s, 6.77 kHz),
- (χ_2,γ_2)=(-237359 Hz/s, 12.63 kHz),
- (χ_3,γ_3)=305176 Hz/s, 16.93 kHz),
- (χ_4,γ_4)=372993 Hz/s, 20.96 kHz).

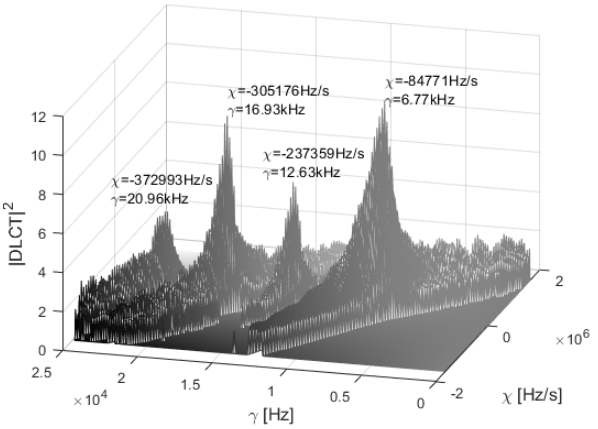

Fig.3. Three-dimensional plot of the $|DLCT|^2$ for a knocking combustion cycle

The above results can be compared with those read from Figure 2. However, because of the limited resolution of the CW distribution, only approximation to the exact values was obtained. The chirp rate parameter χ is related to the rate of the frequency change (which can be read from Fig. 2) by (5). Hence, the approximate values were

χ_1≈-192308/2=-96154 Hz/s,
χ_2≈-481481/2=-240740.5 Hz/s,
χ_3≈-607143/2=-303571.5 Hz/s,
χ_4≈-750000/2=-375000 Hz/s.

The initial frequency of each component was:

γ_1 ≈ 6.7 kHz,
γ_2 ≈ 12 kHz,
γ_3 ≈ 16 kHz,
γ_4 ≈ 20.2 kHz.

By comparing the results, we see that the DLCT was quite accurate. It is important to mention that for real-world signals the peaks in the three-dimensional plot of the $|DLCT|^2$ are not as clearly visible as is the case with ideal LMF signals. This is mainly due to two reasons. Firstly, the signal to be analysed must be the sum of strictly linear chirps (quadratic-phase). For higher-order chirps, the signal representation is not perfectly sparse, that is, the peaks are blurred, and there are large side lobes. Secondly, the background noise affects the performance of the transform.

Experiment 3: This experiment concerns the problem of estimating the chirp parameters in the presence of additive noise. The simulation was run for a monocomponent signal

$$x(t) = e^{j2\pi(\chi t^2+\gamma t)} + n(t) \tag{23}$$

The $n(t)$ is a complex, white Gaussian noise with a zero mean, where Re($n(t)$) and Im($n(t)$) are uncorrelated. The sampling frequency and signal length was f_s=10 kHz, N=1000, respecively. The signal parameters were set to (χ,γ)= (5000 Hz/s, 1 kHz). A computer simulation was conducted for M=250 trials at each noise level, which corresponds to SNRs that ranged from -20 dB to -5 dB (step 0.5 dB). The results of the estimation of the chirp parameters are presented in Figure 4.

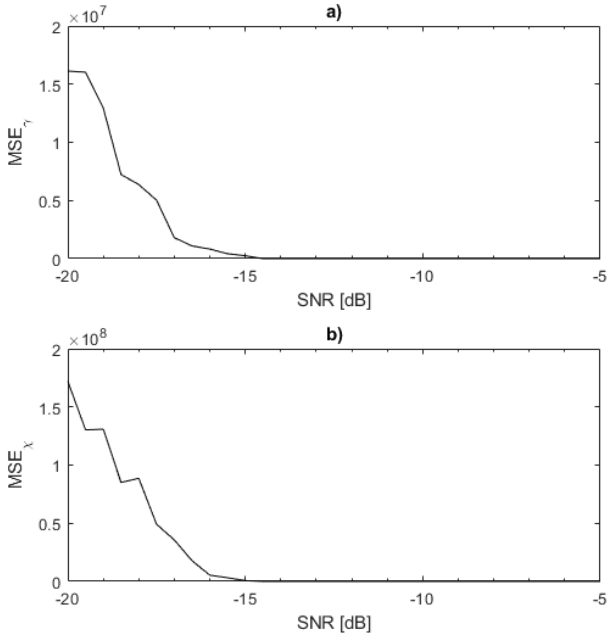

Fig.4. Chirp parameter estimate performance : (a) - initial frequency estimation, (b) - chirp rate estimation

On the y-axis,

$$MSE_\gamma = \frac{1}{M}\sum_{k=1}^{M}\left(\gamma - \hat{\gamma}_k\right)^2 \tag{24}$$

$$MSE_\chi = \frac{1}{M}\sum_{k=1}^{M}\left(\chi - \hat{\chi}_k\right)^2 \tag{25}$$

was plotted, where γ and χ were the assumed values of a parameter, and $\hat{\gamma}_k, \hat{\chi}_k$ - the estimate from the k-th realisation.

One can see that at SNR>-14.5 dB, the MSE of the estimation of the initial frequency reached a zero value. For the chirp rate, the plateau was achieved at SNR>-15 dB. Thus, the presented method performed well for SNR>-14.5 dB, thereby providing a correct chirp parameter estimation even for relatively small SNR values.

The above results are in agreement with the plots shown in Figures 5 and 6.

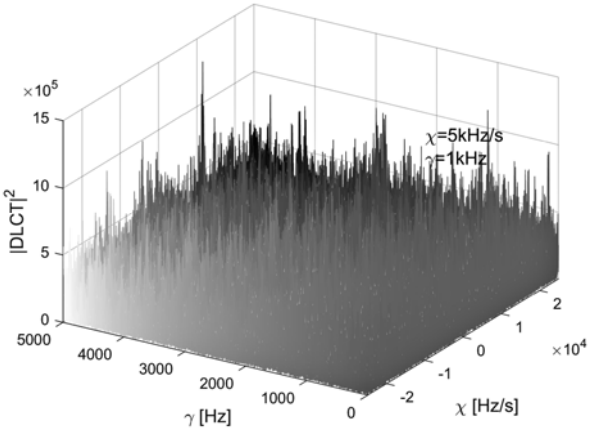

Fig.5. Three-dimensional plot of the $|DLCT|^2$ for a monocomponent signal with SNR= - 20 dB

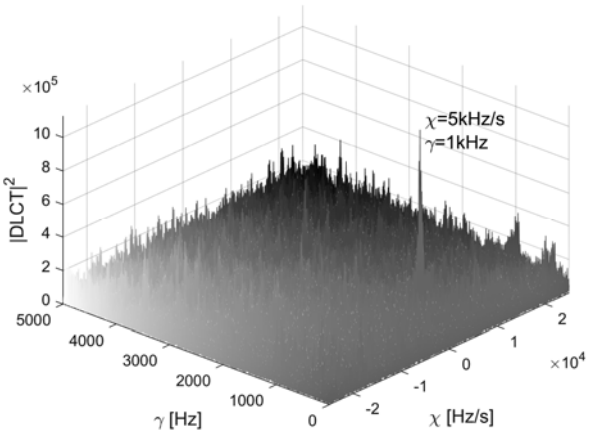

Fig.6. Three-dimensional plot of the $|DLCT|^2$ for a monocomponent signal with SNR= -15 dB

As we can see in Figure 5, when SNR= - 20 dB, the peak that corresponds to the chirp cannot be identified. In contrast to this, when SNR= -15 dB, the peak is clearly visible, providing a correct chirp parameter estimation (Fig. 6).

Conclusions

This paper is focused on estimating the parameters of multicomponent, linear-frequency modulation signals using the discrete linear chirp transform. The presented method offers a simple and efficient solution that delivers a good accuracy with a low computational complexity. The accuracy of the estimation of the chirp ratio and initial frequency were evaluated by simulation experiments, which were conducted on a synthetic multi-component LMF signal and on a real in-cylinder pressure waveform that represents an abnormal combustion process in SI engine. The obtained results are promising and encouraging for the further application of the described method in the field of non-stationary signal processing.

The presented work also opens several areas for further research in this field. Although the DLCT was defined for linear chirps, an interesting direction could be in generalizing the method for higher-order chirps. Moreover, some attempts can be made to develop an automatic algorithm to detect peaks, tailored to the specific form of a three-dimensional plot of the DLCT.

Acknowledgment

This work was supported by the Ministry of Science and Higher Education funding for statutory activities, BK-246/Rau-11/2022.

***Author**: Jerzy Fiołka, PhD, Silesian University of Technology, Faculty of Automatic Control, Electronics and Computer Science, Department of Electronics, Electrical Engineering and Microelectronics, Akademicka 16, 44-100 Gliwice, e-mail: jerzy.fiolka@polsl.pl*

REFERENCES

[1] Djuric P., Kay S., Parameter estimation of chirp signals, *IEEE Trans. Acoust., Speech, Signal Process.*, vol. 38, no. 12, pp. 2118–2126, 1990.

[2] Jensen T., Nielsen J., Jensen J., Christensen M., Jensen S., A fast algorithm for maximum-likelihood estimation of harmonic chirp parameters, *IEEE Trans. Signal Process.*, vol. 65, no. 19, pp. 5137–5152, 2017.

[3] O'Neil J., Flandrin P., Karl W., Sparse representations with chirplets via maximum likelihood estimation, *IEEE Trans. Signal Process.*, no. 48, 1999.

[4] Boashash B., Time-Frequency Signal Analysis and Processing. A Comprehensive Reference. Academic Press, 2015.

[5] Hlawatsch F., Auger F., Time-Frequency Analysis. John Wiley and Sons, 2013.

[6] N. Huang and S. Shen, The Hilbert-Huang Transform and its applications. World Scientific Publishing Co, 2005.

[7] Fiolka J., Application of Hilbert-Huang transform to engine knock detection, *Proceedings of the 20th International Conference Mixed Design of Integrated Circuits and System, MIXDES 2013*, Poland, 2013, pp. 457–461.

[8] Yuan Y., Li Q.-F., Fu Y., Parameters estimation for multicomponent LFM signals using EMD based fractional Fourier transform, *Asia-Pacific Conference on Computational Intelligence and Industrial Applications (PACIIA)*, Wuhan, China, 2009, pp. 488–491.

[9] Fiolka J., Fractional Fourier transform and its application to engine knock detection, *Proceedings of the 22th International Conference Mixed Design of Integrated Circuits and System, MIXDES 2015*, Poland, 2015, pp. 595–598.

[10] Ozaktas H. M., Kutay M. A., Candan C., The fractional Fourier transform with applications in optic and signal processing. John Wiley and Sons, New York, 2001.

[11] Alkishriwo O. A., Phd dissertation: The discrete linear chirp transform and its application," Ph.D. dissertation, University of Pittsburgh, 2012.

[12] Fiolka J., Application of the fractional Fourier transform in automotive system development: The problem of knock detection, *Conference proceedings: Signal Processing Algorithms, Architectures, Arrangements and Applications SPA 2017*, 2017, pp. 286–291.

[13] Capus C., Brown K., Short-time fractional Fourier methods for the time-frequency representation of chirp signals, *J Acoust Soc Am*, 2003.

[14] Alkishriwo O. A., Chaparro L. F., A discrete linear chirp transform (DLCT) for data compression, *11th International Conference on Information Science, Signal Processing and their Applications (ISSPA),* 2012, pp. 1283–1288.

[15] Ferrari G., Internal combustion engines. Esculapio, 2014.

[16] Millo F., Ferraro C., Knock in S.I. engines: A comparison between different techniques for detection and control, *SAE Technical Paper*, 1998, pp. 25–42, 982477.

[17] Iorio B., Giglio V., Police G., Rispoli N., Methods of pressure cycle processing for engine control, *SAE Technical Paper*, 2009, 10.4271/2003-01-0352.

[18] Eriksson L., Thomasso A., Cylinder state estimation from measured cylinder pressure traces - a survey, *20th World Congress, The International Federation of Automatic Control*, 2017.

[19] Fiolka J., Preliminary investigation of the in-cylinder pressure signal using Teager energy operator, *Conference proceedings: Signal Processing Algorithms, Architectures, Arrangements, and Applications SPA 2018*, 2018, pp. 31–36.